

# A STUDY ON THE SEISMIC PERFORMANCE OF SHEAR WALLS UNDER A DYNAMIC LOAD

Tomoki Furuta<sup>1</sup> and Masato Nakao<sup>2</sup>

**KEYWORDS:** Post-and-beam construction system, Plywood shear wall, Braced shear wall, Shake table test

## 1 INTRODUCTION

In recent years, the number of Japanese buildings that have suffered damage due to multiple large earthquakes has increased. As timber buildings do not have an obvious yield point, the shear stiffness of these buildings decreases gradually during the occurrence of multiple earthquakes. Consequently, there is concern about a decrease in seismic performance, which may result in the collapse of timber houses even during relatively small earthquakes. Regarding timber shear walls, to investigate the dynamic performance and to build an analysis model in order to predict earthquake response, several experimental and numerical studies have been conducted, e.g. [1-5]. Nowadays, It has become possible to predict the earthquake response of timber houses. Nevertheless, it remains difficult to predict the earthquake response of timber houses when there are multiple earthquake motions. For this reason, a shake table test of the shear walls of the Japanese post-and-beam construction system was conducted to understand the dynamic characteristics of shear walls during multiple earthquakes. Hysteresis models of the shear walls for earthquake response analysis are proposed using the shake table test results. Moreover, an equivalent linearization method as a simple prediction method for a maximum response displacement was tried.

## 2 SHAKE TABLE TEST

### 2.1 OUTLINE

Specimens for the shake table test were constructed using the Japanese post-and-beam construction system. The wall length of each specimen was 2730 mm, and the specimens contained four columns as shown in Figure 1. Two kinds of shear walls were tested. The first, a plywood shear wall, was 910 mm × 2730 mm in size. A sheet of plywood was nailed to the frame using N50 nails spaced at 150 mm. The second was a braced shear wall, two 45 mm × 90 mm timber braces were attached crosswise to the frame. Conventional brace connectors (C-brace) were used to connect the ends of the braces and the columns. Newly-developed ductile brace connectors (D-brace) were also used as a variation of the braced shear wall.

The new brace connector, as shown in Figure 2, includes a damping mechanism. The thickness of the steel for the connector is 3.2mm. As the lateral displacement of the braced shear wall increases, the bridges deform to absorb a displacement between a column and a brace. Damping force is produced by the plastic deformation of the bridges. The steel core is covered with high-damping rubber to use as a brace connector.

A 15.8 kN weight was applied to the beam (Figure 1). Rollers were arranged along the longitudinal direction of the weight. 25 kN hold-down connectors were installed to reinforce the joint between the ends of the columns and the horizontal members.

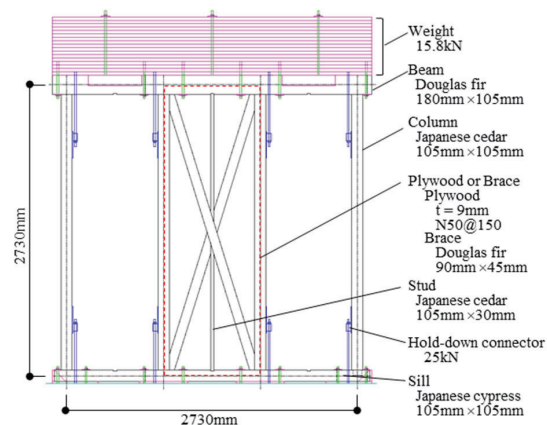


Figure 1: Specimen for the shake table test

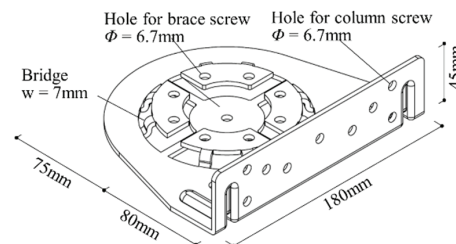


Figure 2: Core of newly-developed ductile brace connector (To use as a brace connector, this steel core is covered with high damping rubber.)

<sup>1</sup> Tomoki Furuta, Nishinippon Institute of Technology, Japan, furuta@nishitech.ac.jp

<sup>2</sup> Masato Nakao, Yokohama National University, Japan, mnakao@ynu.ac.jp

The seismic waves of the 1995 JMA Kobe NS earthquake (as observed at the Kobe branch of the Japan Meteorological Agency on January 17th, 1995) were applied to the specimen. The time history of acceleration and the response acceleration are shown in Figures 3 and 4, respectively.

The input level was stepped up to 80% for the plywood shear wall and up to 100% for the braced shear wall. Before each input step level, 50% of the previous level was applied in order to evaluate the earthquake response characteristics after the stiffness degradation of the shear walls, as shown in Figure 5. In this paper, the step-up input is referred to as "1st", whereas 50% of the previous level input is referred to as "2nd."

Accelerometers were attached to the shake table, the sill, and the beam of the specimens. The story displacement was measured between the beam and the sill.

## 2.2 SHEAR FORCE-DISPLACEMENT RELATIONSHIP AND FAILURE MODE

The shear force-displacement relationship of the plywood shear walls is shown in Figure 6. The shear force  $Q$  was calculated using Equation (1).

$$Q = m \cdot a \quad (1)$$

where  $m$  is mass (16kN/9800mm/sec<sup>2</sup>),  $a$  is acceleration (mm/sec<sup>2</sup>).

A remarkable degradation of shear stiffness was seen under the 40% input load. During the 80% input load, the shear stiffness significantly decreased. Pull-out, punch-

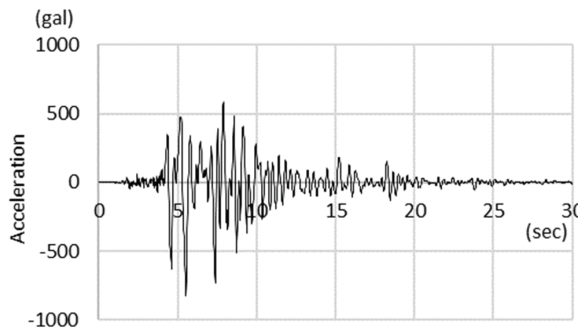


Figure 3: Time history of JMA Kobe NS wave

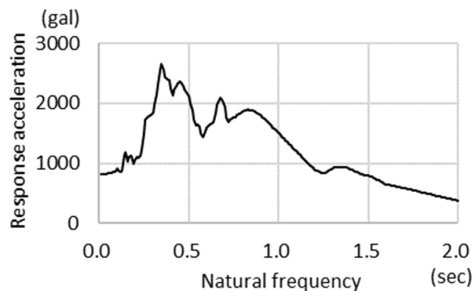


Figure 4: Acceleration response spectrum of JMA Kobe wave (h=5%)

out, and fracture of nails were observed as shown in Figure 7.

For the conventional brace connector, a remarkable decrease in the shear stiffness was observed during the 80% input load as shown in Figure 8. After the application of the 100% input load, as shown in Figure 9, the pull-out of the screws on the column and buckling of the stud were observed.

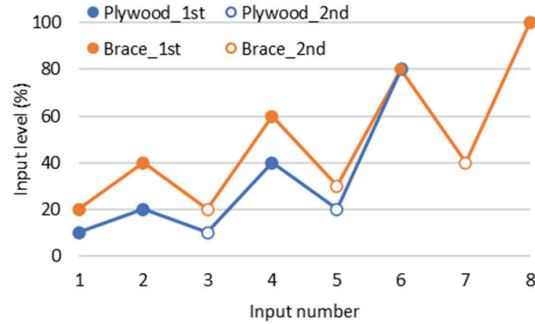


Figure 5: Input level of the JMA Kobe wave

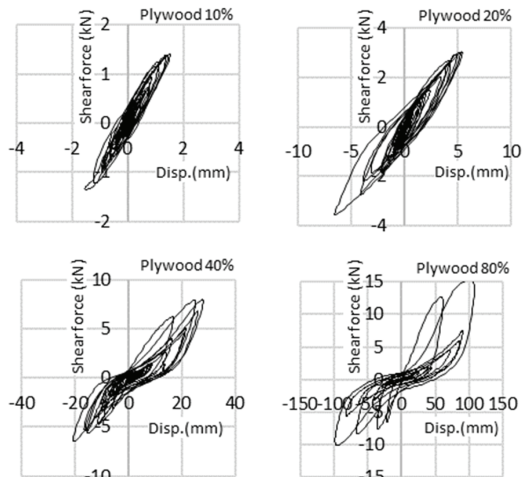


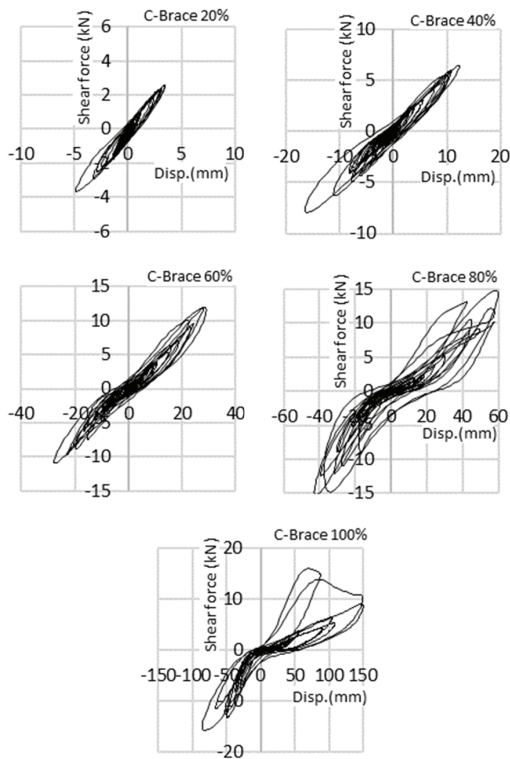
Figure 6: Shear force-displacement relationships of plywood shear wall specimen on each input



Figure 7: Plywood shear wall specimen and nails after the test

No shear stiffness reduction was seen in the shear force-displacement relationship of the braced shear wall with ductile brace connectors during the series of inputs as shown in Figure 10. There was no visible damage to the connectors even after the 100% input load, as shown in Figure 11.

The degradation of the shear stiffness can be found easily from the combined shear force-displacement relationships as shown in Figures 12 to 14. Skeleton curves of the shear force-displacement relationships are shown in Figure 15. The ratio of the shear forces at 1/120 rad for plywood shear wall: braced shear wall with conventional brace connectors: braced shear wall with ductile brace



**Figure 8:** Shear force-displacement relationships of braced shear wall specimen with conventional brace connectors on each input



**Figure 9:** Braced shear wall specimen with conventional brace connectors after the test

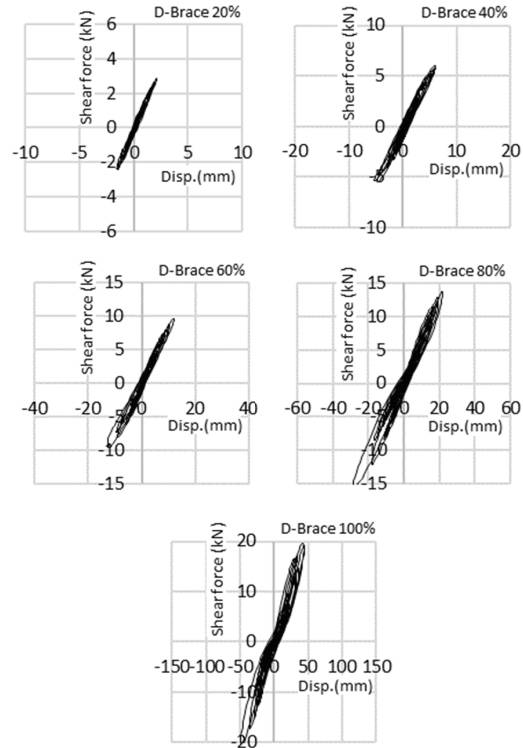


**Figure 10:** Shear force-displacement relationships of braced shear wall specimen with ductile brace connectors on each input

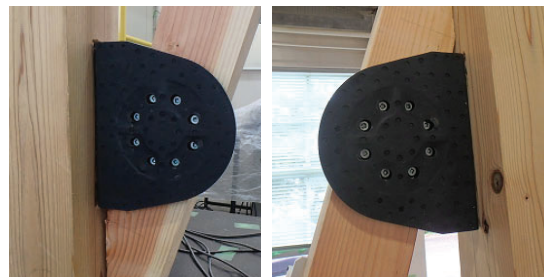


**Figure 11:** Ductile brace connectors after the test

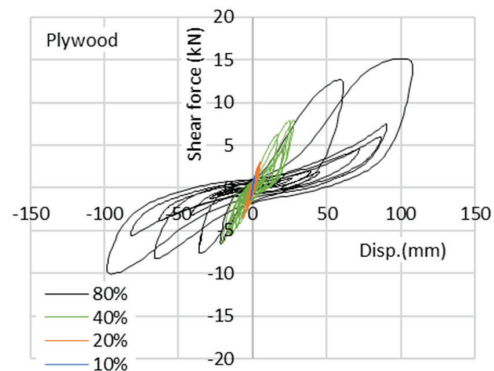


**Figure 12:** Shear force-displacement relationships of plywood shear wall specimen

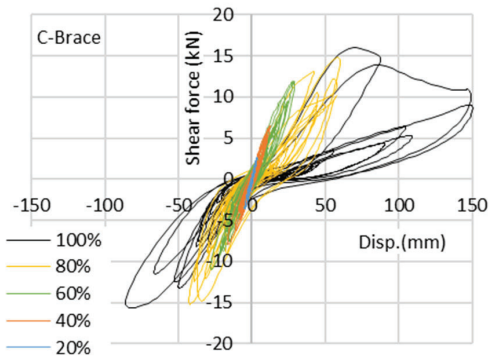


Figure 13: Shear force-displacement relationships of braced shear wall specimen with conventional brace connectors

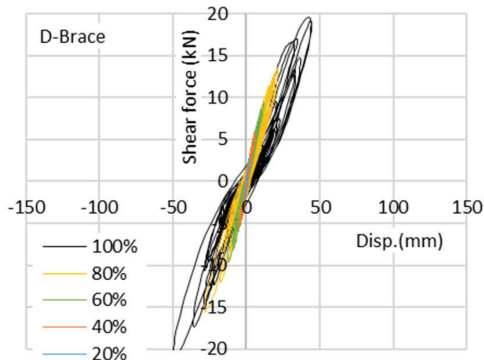


Figure 14: Shear force-displacement relationships of braced shear wall specimen with ductile brace connectors

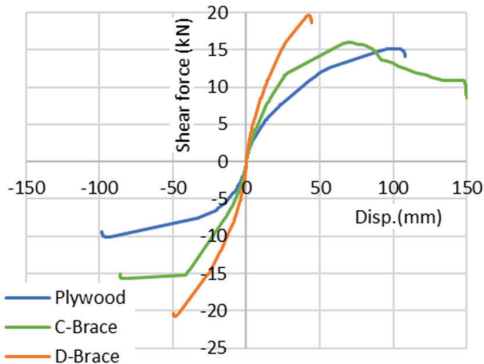


Figure 15: Skeleton curves of shear force-displacement relationships of shear wall specimens

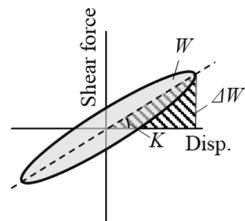


Figure 16: Notations in Equation (2) for calculation of  $H_{eq}$

connectors was 1.0:1.4:2.0. It is obvious that the shear stiffness of the ductile brace connector is superior to the plywood shear wall and the braced shear wall with conventional brace connectors.

### 2.3 TRANSITION OF STRUCTURAL PERFORMANCE OF SPECIMEN

To grasp the structural performance transition of the specimens during a series of loading, the equivalent damping factor ( $H_{eq}$ ) was calculated using Equation (2) on each input load. The notations refer to Figure 16.

$$H_{eq} = \frac{W}{4\pi\Delta W} \quad (2)$$

In addition to that, the shear stiffness of one shear force-displacement loop ( $K$ ) that involves a maximum displacement was calculated. For a comparison, initial stiffness ( $K_0$ ) was also calculated on each input load. The amplitude of one loop picked out for the calculation was approximately 0.5mm to 1.0mm.

Figure 17 shows the structural performance transition of the plywood shear wall. It is found that the  $H_{eq}$  is about 15% regardless of input level. It is also found that the

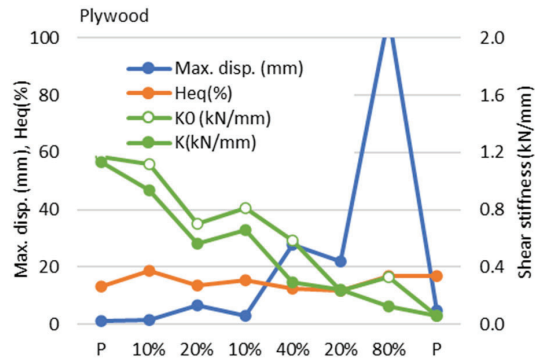


Figure 17: Maximum displacement, equivalent damping factor ( $H_{eq}$ ), shear stiffness  $K_0$  and shear stiffness  $K$  of plywood shear wall specimen

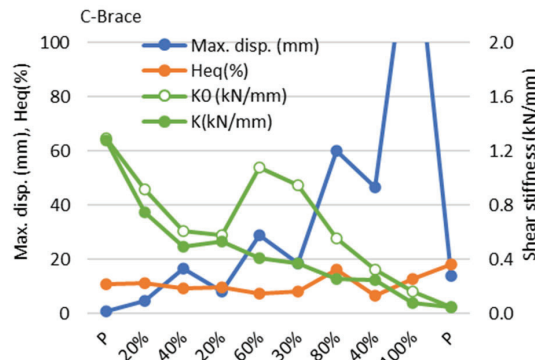


Figure 18: Maximum displacement, equivalent damping factor ( $H_{eq}$ ), shear stiffness  $K_0$  and shear stiffness  $K$  of braced shear wall specimen with conventional brace connectors



shear stiffness decreases as the maximum displacement increases. In terms of  $K_0$ , it is larger than  $K$  during a series of input loads.

Figure 18 shows the ones of the braced shear wall with convention brace connectors.  $H_{eq}$  is about 10 to 15% through the series of input loads. It is also found that the shear stiffness decreases as the maximum displacement increases same as the plywood shear wall. Unlike the plywood shear wall, the difference between  $K$  and  $K_0$  is relatively large. It implies that the degradation of shear stiffness of the braced shear wall with convention brace fasteners is remarkable.

Figure 19 shows the ones of the braced shear wall with ductile brace connectors.  $H_{eq}$  is about 10%, it is lower than the plywood shear wall and the braced shear wall with conventional brace connectors. As in the previous Figure 14, the braced shear wall with the ductile brace connectors was almost elastic during the series of input loads, it is considered that damping due to plasticity is not contained in  $H_{eq}$ . Moreover,  $K_0$  is close to  $K$ , and degradation of shear stiffness is considered to be little.

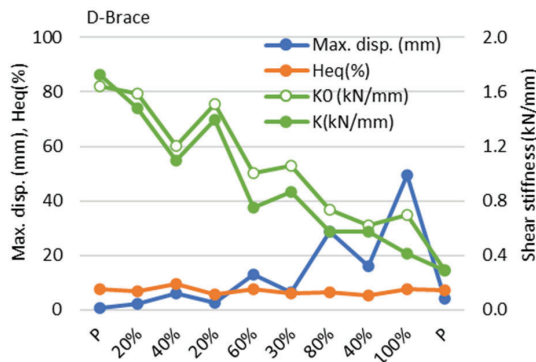


Figure 19: Maximum displacement, equivalent damping factor ( $H_{eq}$ ), shear stiffness  $K_0$  and shear stiffness  $K$  of braced shear wall specimen with ductile brace connectors

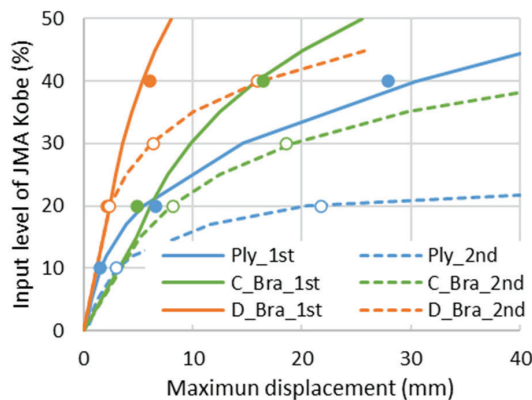


Figure 20: Maximum displacement for different input levels

## 2.4 EFFECT OF MULTIPLE INPUTS

Figure 20 shows the relationship between the input level of the JMA Kobe NS wave and the maximum response displacement of the shear walls. The regression curves for the 1st and 2nd inputs are also indicated in the figure. For the plywood shear wall, the 2nd displacement at 10% input was twice that of the 1st displacement. The 2nd displacement of the braced shear wall with ductile brace connectors exceeded that of the 1st displacement at an input over 20%, whereas the 2nd displacement of the braced shear wall with conventional brace connectors exceeded that of the 1st displacement at an input over 15%. From the regression curves, it can be seen that the response displacement of the 2nd input increases rapidly with the input level.

Figure 21 shows the relationship between the maximum displacement and the natural period of the three shear walls, where the maximum displacements were divided by the input level to convert to the one under 100% wave. The displacement response spectrums of the JMA Kobe NS 100% wave with 10%, 15%, and 20% damping ratio is also displayed in the figure. The natural period  $T$  was calculated using the mass,  $m=16\text{kN/g}$  ( $g=9800\text{mm/sec}^2$ ), and shear stiffness,  $K(\text{kN/mm})$ .

$$T = 2\pi \sqrt{\frac{m}{K}} \quad (3)$$

Most of the maximum displacements are located between the displacement response spectrums of damping ratios of 15% and 20%. There is no remarkable difference between 1st and 2nd inputs. From the figure, it is found that a maximum response displacement can be estimated using the natural period based on  $K$  and the displacement response spectrum. Suppose the displacement response spectrum of a 15% damping ratio is used, predicted

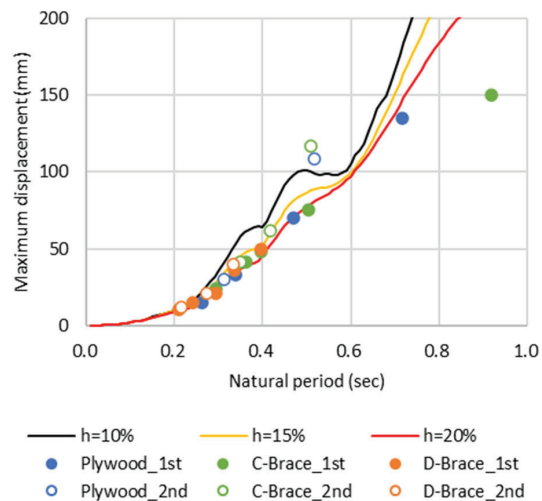


Figure 21: Relationship between maximum displacement and natural period based on shear stiffness  $K$

response displacement would be the safe side for the three shear walls.

However, there is an issue that for predicting a maximum response displacement using a displacement response spectrum, it is impossible to grasp  $K$  beforehand because  $K$  is let from a maximum response displacement.

### 3 RESPONSE DISPLACEMENT PREDICTION

#### 3.1 EARTHQUAKE RESPONSE ANALYSIS

On the basis of the shake table test results, hysteresis models of the plywood shear wall and the braced shear wall were set as shown in Figures 22 to 24. Earthquake response analysis was conducted using input waves on the shake table test. 16kN of weight and 10% of viscous damping were applied to single degree of freedom analysis model.

Figures 25 to 27 show maximum response displacements. A comparison of the earthquake response analysis using the hysteresis models and the shake table test results shows that the maximum response displacements of the analysis and the shake table test showed a good degree of correspondence in a small displacement range. In a large displacement range, there is a relatively large difference, which implies that more parameters of the hysteresis model are needed to predict maximum response displacements accurately in a wide displacement range.

#### 3.2 EQUIVALENT LINEARIZATION METHOD

There was an issue that  $K$  derived from the maximum response displacement is needed to calculate the natural period for the prediction of maximum response displacement using a displacement response spectrum. As one solution for the above-expressed issue, in place of  $K$ , there is a possibility that  $K_0$  is rather useful for the prediction of a maximum response displacement because  $K_0$  can be calculated based on approximately 0.5mm to 1mm of amplitude. If time history data of displacement and acceleration could be recorded even under relatively small input,  $K_0$  can be calculated.

Figure 28 shows the relationship between the natural period calculated using  $K_0$  and the maximum displacement of the shear walls, where the maximum displacements were converted to the one under 100% wave. The displacement response spectrum of the JMA Kobe NS 100% wave with a 5% damping ratio is added to the figure as well as 10%, 15%, and 20%. Most of the maximum displacements of the shear walls are located near the displacement response spectrum of a 5% damping ratio, which implies that the response displacement can be predicted using the natural period based on  $K_0$  regardless of the 1st or 2nd input.

Comparing the experimental maximum displacements and the displacement response spectrum, most of the maximum displacement was lower than the displacement response spectrum. Therefore, safe side prediction regarding maximum displacements is expected.

In case displacement and acceleration data can't be obtained, to grasp  $K_0$  for the prediction of a maximum

response displacement, it is valid to make use of the largest displacement in experienced displacements so far because there is a close relationship between the largest displacement in the past and  $K_0$ .

Figure 29 shows the relationship between the shear stiffness degradation ratio and the maximum displacement. The x value of each point is the largest

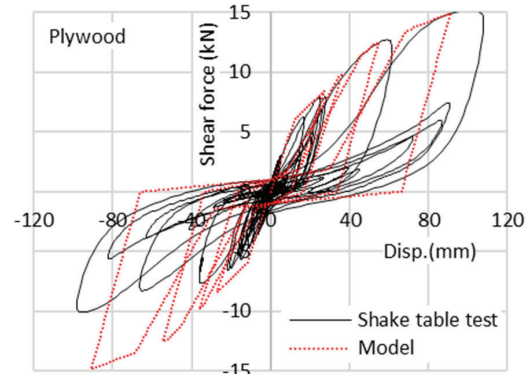


Figure 22: Shear force-displacement relationship model of plywood shear wall

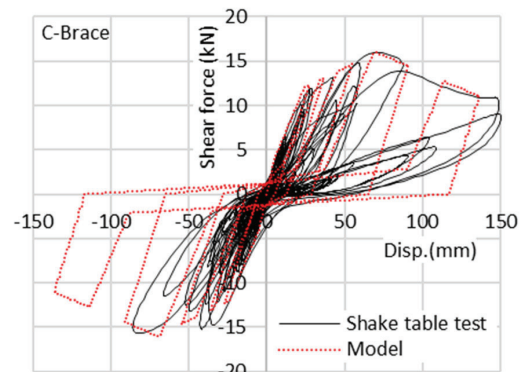


Figure 23: Shear force-displacement relationship model of braced shear wall with conventional brace connectors

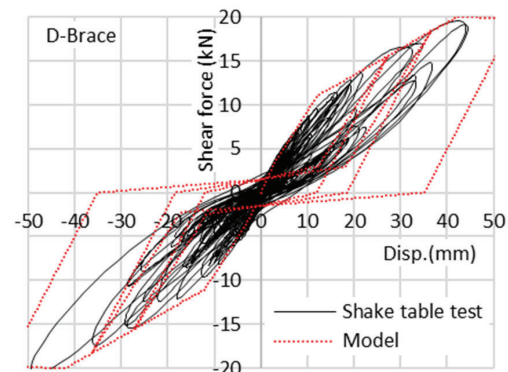


Figure 24: Shear force-displacement relationship model of braced shear wall with ductile brace connectors

displacement up to the time, and the y value, shear stiffness degradation ratio, is a ratio of the shear stiffness ( $K_0$ ) after the input load where the largest displacement is recorded to the initial shear stiffness. Ignoring the difference of 1st and 2nd inputs, regression lines according to the points belonging to each shear wall are also indicated in the figure. Equations (4), (5), and (6) represent regression lines of the plywood shear wall, the braced shear wall with conventional brace connectors, and the braced shear wall with ductile brace connectors, respectively.

$$y = x^{-0.4} - x/1000 \quad (4)$$

$$y = x^{-0.25} - x/500 \quad (5)$$

$$y = x^{-0.22} - x/500 \quad (6)$$

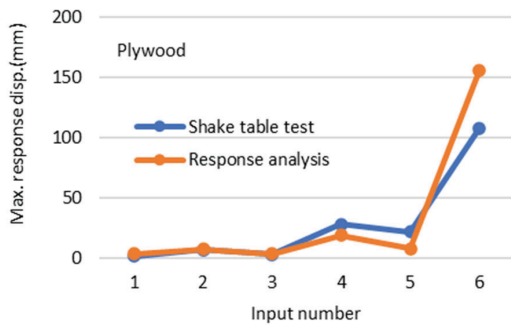


Figure 25: Maximum response displacement of plywood shear wall

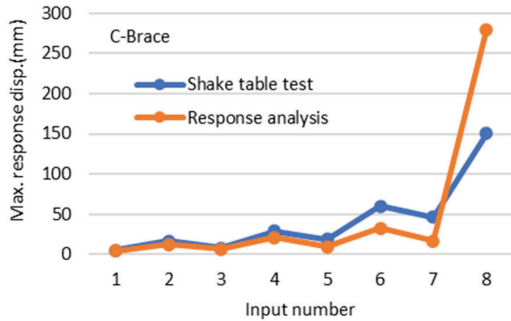


Figure 26: Maximum response displacement of braced shear wall with conventional brace connectors

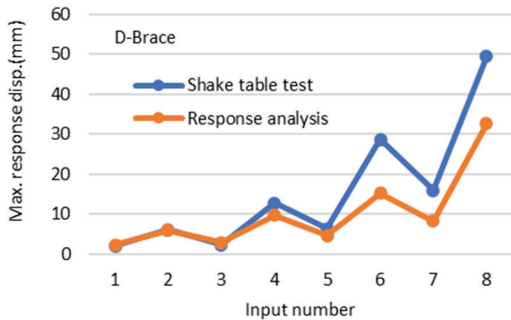


Figure 27: Maximum response displacement of braced shear wall with ductile brace connectors

In the case that the experienced largest displacement is known, the ratio of stiffness can be found using the equations, and  $K_0$  can be calculated by multiplying the initial stiffness of the shear wall and the ratio of stiffness. Furthermore, using the displacement response spectrum of a 5% damping ratio, a maximum response displacement under the next input wave can be predicted. Figures 30 to 32 show maximum response displacements. Though the equivalent linearization method is simple, predicted response displacements are close to the maximum displacements obtained by the shake table test. With the derived regression curves from the shake table test results, the equivalent linearization method is

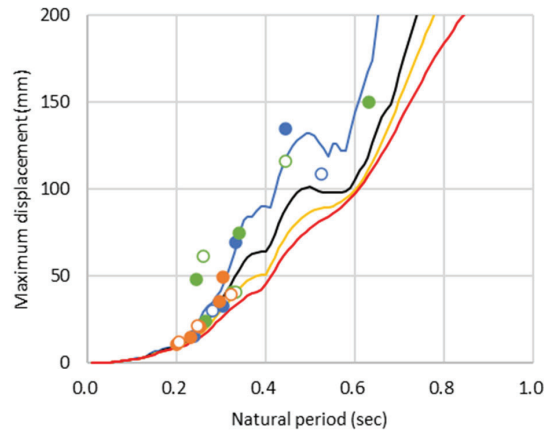


Figure 28: Relationship between maximum displacement and natural period based on shear stiffness  $K_0$

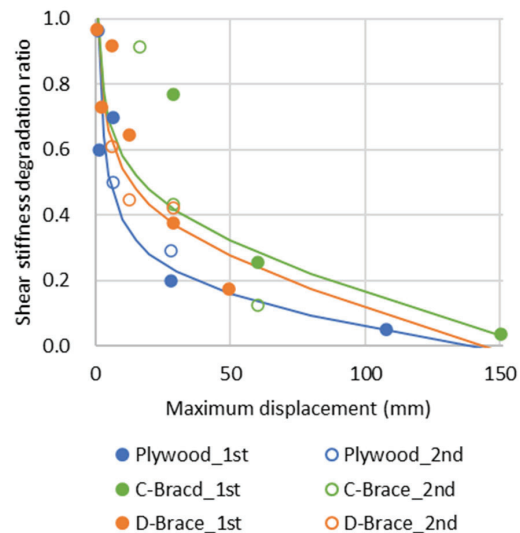
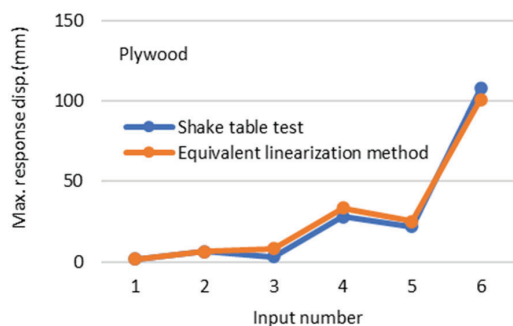
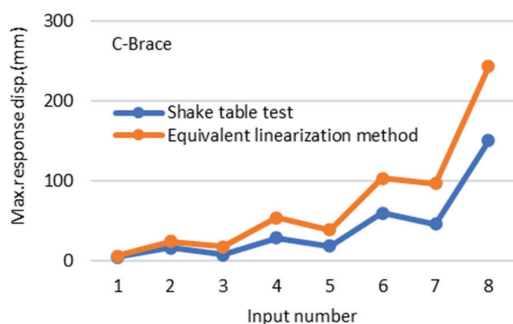


Figure 29: Relationship between shear stiffness degradation ratio to initial shear stiffness and maximum displacement



**Figure 30:** Maximum response displacement of plywood shear wall



**Figure 31:** Maximum response displacement of braced shear wall with conventional brace connectors

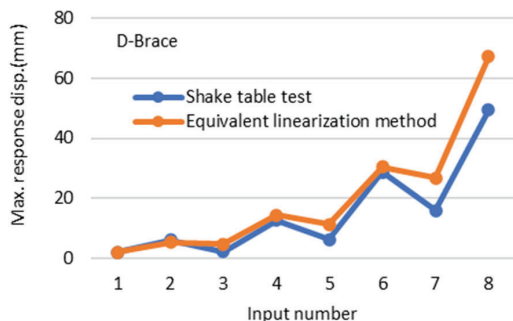


**Figure 32:** Maximum response displacement of braced shear wall with ductile brace connectors

considered to be a useful method to predict maximum response displacements even under multiple input waves.

#### 4 CONCLUSIONS

Shake table tests of a plywood shear wall and braced shear walls were conducted to understand their dynamic characteristics under multiple earthquake inputs. Moreover, hysteresis models of the shear walls were proposed based on the shake table test results, and earthquake response analysis was conducted. The maximum response displacements from the analysis results were relatively close to the shake table test results in a small displacement range. Additionally, an equivalent linearization method as a simple prediction method for a

maximum response displacement was tried. Using the initial shear stiffness and the shear stiffness degradation ratio derived from the shake table test results, the prediction results showed good correspondence with the shake table test results.

#### ACKNOWLEDGEMENT

Authors express our gratitude for the great support on the shake table test by Dr. Hideo Fujitani and Dr. Yoichi Mukai of Kobe university.

#### REFERENCES

- [1] Nobuyoshi Yamaguchi, Chikahiro Minowa, and Masashi Miyamura: Seismic Performance of Wooden Shear Walls on Dynamic Condition. Proceedings of 12th World Conference on Earthquake Engineering, 2000
- [2] Jennifer Durham, Frank Lam, and Helmut G. L. Prion: Seismic Resistance of Wood Shear Walls with Large OSB Panels. Journal of Structural Engineering, 127(12), 1460-1466, 2001
- [3] John W. van de Lindt, Hongyan Liu, and Shiling Pei: Performance of a Woodframe Structure during Full-Scale Shake-Table Tests: Drift, Damage, and Effect of Partition Wall. Journal of Performance of Constructed Facilities, 21(1), 35-43, 2007
- [4] Erol Varoglu, Erol Karacabeyli, Siegfried Stiemer, Chun Ni, Marlen Buitelaar, and Dan Lungu: Midply Wood Shear Wall System: Performance in Dynamic Testing. Journal of Structural Engineering, 133(7), 1035-1042, 2007
- [5] C. Boudaud, J. Humbert, J. Baroth, S. Hameury, and L. Daudeville: Joints and wood shear walls modelling II: Experimental tests and FE models under seismic loading. Engineering Structures, 101, 743-749, 2015